Research Article

Zbigniew Lozia and Piotr Zdanowicz*

Simulation assessment of the half-power bandwidth method in testing shock absorbers

https://doi.org/10.1515/eng-2021-0011
Received Jul 13, 2020; accepted Sep 28, 2020

Abstract: The work deals with usability of the half-power bandwidth method in the diagnostic testing of automotive shock absorbers. In all the simulation tests, the front and rear suspension system of a present-day medium-class motor car was considered. At the first stage, calculations were made in the frequency domain for a linear "quarter-car" model with two degrees of freedom; then, simulations were carried out in the time domain with using a similar but strongly nonlinear model. In the latter case, actual characteristics (corresponding to those obtained from test rig measurements) of shock absorber damping, suspension and tire elasticity, sliding friction in the suspension, and "wheel hop" were considered. The calculations were carried out every time for twelve levels of viscous damping in the suspension system, which made 48 calculation series in total. The factors of gain in the vertical force between the tester's vibration plate and the vehicle tire (relative to the input force applied) and the dimensionless coefficients of viscous damping in the suspension system, determined by the half-power bandwidth method, were thoroughly analyzed. The calculation results were presented in graphical form. Attention was also paid to the distortions caused by the force of inertia of the tester's vibration plate.

Keywords: suspension, damping coefficient, peak-picking method

1 Introduction

The technical condition of automotive shock absorbers is essential for vehicle motion safety and occupants' comfort. With the development of damping components of suspension systems, newer and better methods of diagnosing such parts are sought. The "on-vehicle" tests are particularly useful thanks to their low cost and short time. Predominantly, "forced vibration tests" are used for this purpose [1, 2]. At present, efforts are made to adopt in Europe a uniform (standard) method of forcing the vibration for all the shock absorber testers. As one of the peculiarities of such a method, the stroke of the tester's vibration plate is to be constant, equal to *e.g.* 6 mm, as it is in the case of the EUSAMA machines [1–4]. Unfortunately, such testers, which are most popular, suffer from a major drawback: the final test result strongly depends on tire inflation pressure (*i.e.* tire stiffness), sprung mass, sliding friction in the suspension system, test conditions, and tester characteristics [1, 2, 4, 5]. In consideration of the above, the authors, when searching for new "on-vehicle" shock absorber assessment methods and having reviewed the literature, paid particular attention to publications [3, 6], where a suggestion was made to introduce some modifications to the EUSAMA testers and to use the half-power bandwidth method for determining the dimensionless coefficients of damping in the motor vehicle suspension system. This method is derived from modal analysis [7]. However, it is applied to systems with a single degree of freedom and with low damping (where the dimensionless damping coefficients are below 0.1 – see also *e.g.* [8]). The authors decided to assess the usability of this method in diagnostic testing of automotive suspension systems, where the relative damping coefficient reaches and even exceeds a value of 0.3. A novelty in relation to publications [3, 6] is here the use of a linear and a strongly nonlinear quarter-car model.

2 The half-power bandwidth method in the testing of automotive shock absorbers

The authors of publication [3] have shown that the said half-power bandwidth method [7] may be used to deter-

***Corresponding Author: Piotr Zdanowicz:** Warsaw University of Technology, Faculty of Transport, Koszykowa Street 75, 00-662 Warsaw, Poland; Email: piotr.zdanowicz@pw.edu.pl
Zbigniew Lozia: Warsaw University of Technology, Faculty of Transport, Koszykowa Street 75, 00-662, Warsaw, Poland; Łukasiewicz Research Network – Automotive Industry Institute PIMOT, Jagiellońska Street 55, 03-301 Warsaw, Poland; Email: zbigniew.lozia@pw.edu.pl

mine the dimensionless coefficient of damping in the suspension system. They used a modified EUSAMA tester (with a system to measure the vertical force under the vibration plate, at a sinusoidal input with a constant amplitude of 3 mm), but with the test duration time being significantly extended (to 140 s). Thus, small changes in the input frequency were obtained (from 25 Hz to 0, with a rate of 0.18 Hz/s) and, in consequence, quasi-state conditions of motion were ensured for the core phase of the test. Additionally, the vertical displacement of the tester's vibration plate was measured. Thus, with using the fast Fourier transform, factors of gain in the vertical force measured under the EUSAMA tester's vibration plate (relative to the input force), *i.e.* the absolute values of their transmittance (for linear systems), may be determined. By analyzing the curves representing these quantities close to the second natural frequency of the undamped system and with using the half-power bandwidth method (Figure 1), the estimated value of the coefficient of viscous damping in the motor vehicle suspension system may be determined from formula (1) [3, 7]:

$$\vartheta_{C1} = \frac{f_{C2}^2 - f_{C1}^2}{4 \cdot f_{Cm}^2} \tag{1}$$

where: f_{Cm} is the frequency corresponding to the maximum value of the factor of gain in the force measured in the tester ($HFDZ_{max}$) and f_{C1} and f_{C2} are the frequencies corresponding to the value $HFDZ_{max}/\sqrt{2}$ (see Figure 1).

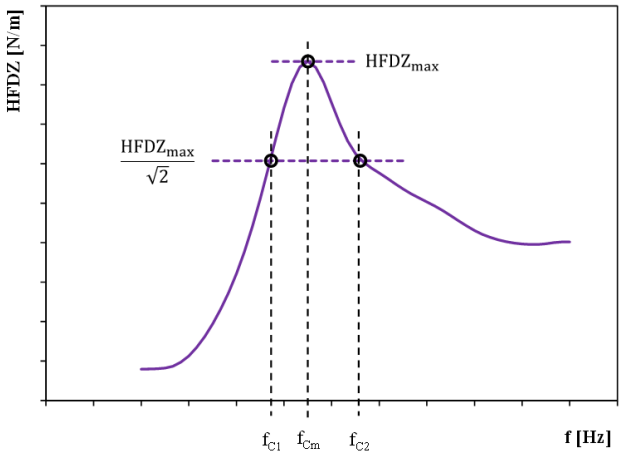

Figure 1: Illustration showing the characteristic points of the factor of gain in the force measured in the tester (HFDZ) in the half-power bandwidth method

The considerations presented in publication [3] were continued in [6] (by the same authors). It was ascertained that shock absorbers might be tested with making use of the effect of amplification of the vertical force (measured under the tester's vibration plate) in the resonance area, for the first natural frequency. In this connection, the input frequency should decline in the core phase of the test from 3 Hz to 0 for a period of 30 s (with a rate of 0.1 Hz/s). For the suspension deflection rates during the test to be similar to those occurring in typical road conditions, the amplitude of the sinusoidal input was increased to 12.5 mm. Additionally, an assumption was made that the curves used as characteristics of the factor of gain in the force measured in the tester were symmetrical and, therefore, a simplified equation (2) might be applied here:

$$\vartheta_{C2} = \frac{f_{C2} - f_{C1}}{2 \cdot f_{Cm}} \approx \vartheta_{C1} \tag{2}$$

3 Simulation models used

The usability of the half-power bandwidth method in the diagnostic testing of automotive shock absorbers was assessed in two stages. At first, simulations were carried out in the frequency domain with using a linear quarter-car model placed on a suspension tester (Figure 2a). Next, time domain simulations were performed using an analogous, highly non-linear model (Figure 2b and 2c).

3.1 Linear model

In this representation (Figure 2a), sprung mass m_1, unsprung mass m_2, and mass m_3 of tester's vibration plate were taken into account. The vertical displacements of model bodies relative to their equilibrium positions (for the exciter, *i.e.* the vibration plate, being in its rest position) are denoted here by z_1 and z_2; ζ is the time-varying kinematic input applied by the exciter. The stiffness and damping of the suspension system are denoted by k_1 and c_1, respectively, and the radial stiffness and damping of the tire are denoted by k_2 and c_2, respectively. To check the distorting impact of the inertia of tester's vibration plate (exciter) on the final shock absorber test results, the dynamic component of the normal reaction at the tire-exciter contact point (F_{dz}) and the dynamic component of the force measured in the tester (F_{md}) were distinguished.

The equations of motion were derived in accordance with the principle of dynamic force analysis (see [9]), with taking into account the forces of inertia of individual mass elements. The equations in their full and concise matrix

form have been shown below (3):

$$\begin{bmatrix} m_1 & 0 \\ 0 & m_2 \end{bmatrix} \cdot \begin{bmatrix} \ddot{z}_1 \\ \ddot{z}_2 \end{bmatrix} + \begin{bmatrix} c_1 & -c_1 \\ -c_1 & c_1 + c_2 \end{bmatrix} \cdot \begin{bmatrix} \dot{z}_1 \\ \dot{z}_2 \end{bmatrix} + \quad (3)$$
$$+ \begin{bmatrix} k_1 & -k_1 \\ -k_1 & k_1 + k_2 \end{bmatrix} \cdot \begin{bmatrix} z_1 \\ z_2 \end{bmatrix} = \begin{bmatrix} 0 \\ c_2 \end{bmatrix} \cdot \dot{\zeta} + \begin{bmatrix} 0 \\ k_2 \end{bmatrix} \cdot \zeta$$
$$M \cdot \ddot{q} + C \cdot \dot{q} + K \cdot q = C_\zeta \cdot \dot{\zeta} + K_\zeta \cdot \zeta$$

where: M, C, K, C_ζ, and K_ζ are, respectively, the matrices of inertia, viscous damping, stiffness, and matrices representing the excitation impact exerted through the tire damping and the radial stiffness of the tire; q, $\dot{q}$, and $\ddot{q}$ are the vectors of generalized displacements, velocities, and accelerations, respectively.

The Laplace transform of (3) at zero initial conditions and some subsequent transformations have resulted in the obtaining of equation (4) and its solution (5):

$$\left(M \cdot s^2 + C \cdot s + K\right) \cdot q(s) = \left(C_\zeta \cdot s + K_\zeta\right) \cdot \zeta(s) \quad (4)$$

$$q(s) = \left(M \cdot s^2 + C \cdot s + K\right)^{-1} \cdot \left(C_\zeta \cdot s + K_\zeta\right) \cdot \zeta(s) \quad (5)$$

The operational transmittances (transfer functions) for displacements, velocities, and accelerations were expressed by relations (6), (7), (8) as the ratios of the Laplace transform of the output signal to the Laplace transform of the input signal (excitation):

$$H_q(s) = \begin{bmatrix} H_{q_1}(s) \\ H_{q_2}(s) \end{bmatrix} = \frac{q(s)}{\zeta(s)} = \quad (6)$$
$$= \left(M \cdot s^2 + C \cdot s + K\right)^{-1} \cdot \left(C_\zeta \cdot s + K_\zeta\right)$$

$$H_{\dot{q}}(s) = \begin{bmatrix} H_{\dot{q}_1}(s) \\ H_{\dot{q}_2}(s) \end{bmatrix} = \frac{\dot{q}(s)}{\zeta(s)} = s \cdot H_q(s) \quad (7)$$

$$H_{\ddot{q}}(s) = \begin{bmatrix} H_{\ddot{q}_1}(s) \\ H_{\ddot{q}_2}(s) \end{bmatrix} = \frac{\ddot{q}(s)}{\zeta(s)} = s^2 \cdot H_q(s) \quad (8)$$

To pass from the Laplace transform to the Fourier transform, it will be enough to pass from domain s to parameter $i \cdot \omega$ (with assuming that the real part is equal to zero). For the linear model used here, the Fourier transform of the dynamic component of the vertical force at the tire-exciter contact point was described by (9):

$$F_{dz}(i \cdot \omega) = c_2 \cdot \left[\dot{\zeta}(i \cdot \omega) - \dot{z}_2(i \cdot \omega)\right] + \quad (9)$$
$$+ k_2 \cdot \left[\zeta(i \cdot \omega) - z_2(i \cdot \omega)\right]$$

Based on equations (6)–(9) and in result of appropriate transformations, a compact end form of the spectral transmittance for the dynamic vertical force at the tire-exciter contact point was finally obtained (with remembering that $q_1 = z_1$ and $q_2 = z_2$):

$$H_{Fdz}(i \cdot \omega) = \frac{F_{dz}(i \cdot \omega)}{\zeta(i \cdot \omega)} = \quad (10)$$
$$= (i \cdot c_2 \cdot \omega + k_2) \cdot \left[1 - H_{q_2}(i \cdot \omega)\right]$$

The difference between the dynamic component of the force measured in the tester (F_{md}) and the dynamic vertical force at the tire-exciter contact point (F_{dz}) arises from the force of inertia of tester's vibration plate (exciter):

$$H_{Fmd}(i \cdot \omega) = \frac{F_{md}(i \cdot \omega)}{\zeta(i \cdot \omega)} \quad (11)$$
$$H_{Fmd}(i \cdot \omega) = \frac{F_{dz}(i \cdot \omega) + m_3 \cdot \ddot{\zeta}(i \cdot \omega)}{\zeta(i \cdot \omega)}$$
$$H_{Fmd}(i \cdot \omega) = \frac{F_{dz}(i \cdot \omega) - m_3 \cdot \omega^2 \cdot \zeta(i \cdot \omega)}{\zeta(i \cdot \omega)}$$
$$H_{Fmd}(i \cdot \omega) = (i \cdot c_2 \cdot \omega + k_2) \cdot \left[1 - H_{q_2}(i \cdot \omega)\right] - m_3 \cdot \omega^2$$
$$H_{Fmd}(i \cdot \omega) = H_{Fdz}(i \cdot \omega) - m_3 \cdot \omega^2$$

The quantities describing the properties of the linear model, *i.e.* the Hertz and radian natural frequency ($f_{01/02}$ and $\omega_{01/02}$, respectively) of the undamped system (12), critical damping coefficient c_{kr1} (13), and relative damping coefficient ϑ_1 (14) were also used:

$$\omega_{01/02}^2 = \frac{k_1 \cdot m_2 + (k_1 + k_2) \cdot m_1}{2 \cdot m_1 \cdot m_2} \mp \quad (12)$$
$$\mp \sqrt{\left[\frac{k_1 \cdot m_2 + (k_1 + k_2) \cdot m_1}{2 \cdot m_1 \cdot m_2}\right]^2 - \frac{k_1 \cdot k_2}{m_1 \cdot m_2}} =$$
$$= \left(2\pi \cdot f_{01/02}\right)^2$$

$$c_{kr1} = 2 \cdot \sqrt{\frac{k_1 \cdot k_2 \cdot m_1}{k_2 + k_1 \cdot \left(1 + \frac{m_2}{m_1}\right)}} \quad (13)$$
$$c_{kr1} \approx 2 \cdot \sqrt{\frac{k_1 \cdot k_2 \cdot m_1}{k_2 + k_1}} \quad \text{for} \quad m_1 \gg m_2$$

$$\vartheta_1 = \frac{c_1}{c_{kr1}} \quad (14)$$

3.2 Nonlinear model

At the second stage, numerical computations were carried out in the time domain with using a strongly nonlinear quarter-car model (Figure 2b and 2c). Force F_{st} balances the weight of system masses ($m_1 \cdot g$, $m_2 \cdot g$, $m_3 \cdot g$). The dynamic components F_{md} and F_{dz} were taken separately to compare the results obtained for the two models.

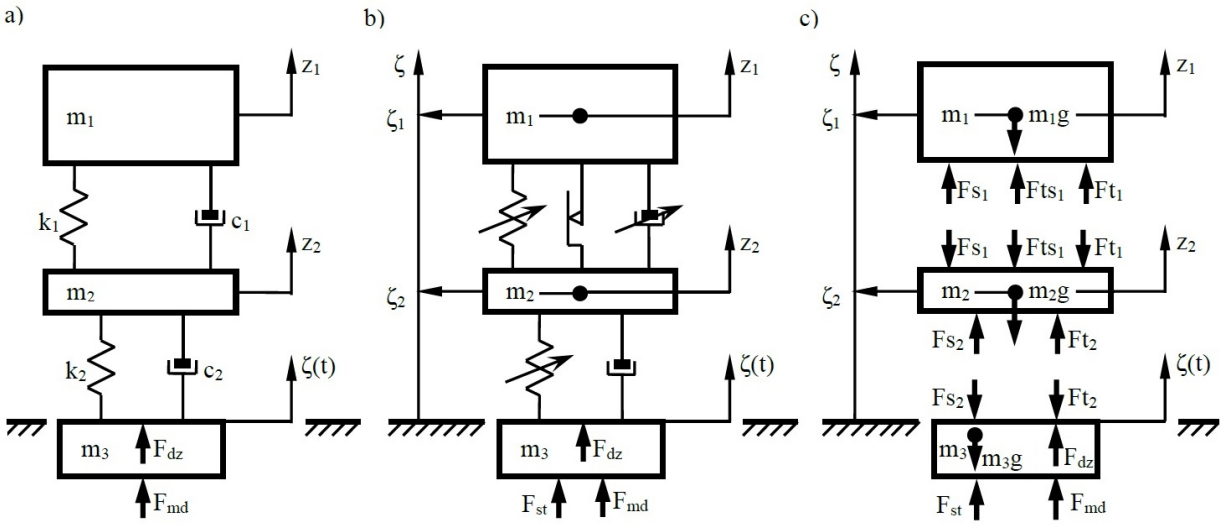

Figure 2: Quarter-car model on a diagnostic shock absorber tester: a) general structure of linear version; b) general structure of nonlinear version; c) force system in nonlinear version

The actual elasticity characteristics of vehicle suspension and tires, sliding friction in the suspension system, and tire separation from the ground were taken into account. The description of these properties was exactly consistent with the results of test rig measurements of the real system. The equations of motion (15) of the nonlinear quarter-car model were derived according to the principle of dynamic force analysis.

$$\begin{cases} \ddot{\zeta}_1 = \frac{Fs_1+Fts_1+Ft_1}{m_1} - g \\ \ddot{\zeta}_2 = \frac{-Fs_1-Fts_1-Ft_1+Fs_2+Ft_2}{m_2} - g \end{cases} \tag{15}$$

where: $\ddot{\zeta}_1$ and $\ddot{\zeta}_2$ are accelerations of the sprung and unsprung mass; Fs_1, Fts_1, and Ft_1 are forces of elasticity, sliding friction, and viscous damping in the suspension system; Fs_2 and Ft_2 are forces of elasticity and damping in the tire; and g is acceleration of gravity.

The elasticity force in the suspension system was approximated by a linear function and a 2nd or 3rd degree polynomial:

$$Fs_1 = \begin{cases} A1s_1 \cdot u_1 & \text{for } u_1 \le u_{1gr} \\ A2s_1 \cdot u_1^3 + B2s_1 \cdot u_1^2 + & \\ +C2s_1 \cdot u_1 + D2s_1 & \text{for } u_1 > u_{1gr} \end{cases} \tag{16}$$

where: $A1s_1$ and $A2s_1$ to $D2s_1$ are coefficients of the functions that describe the elasticity force in the suspension system at low and high deflection values, respectively; u_{1gr} is boundary between areas of different descriptions of the elasticity force; u_1 is deflection of the suspension system, according to (17):

$$u_1 = \zeta_2 - \zeta_1 + om_0 \tag{17}$$

where: om_0 is the difference between coordinates ζ_1 and ζ_2 at which $Fs_1 = 0$.

The force of sliding friction in the suspension system is represented as follows:

$$Fts_1 = \begin{cases} Ats_1 \cdot sgn\, \dot{u}_1 & \text{for } |\dot{u}_1| > \dot{u}_{1gr} \\ Ats_1 \cdot \frac{\dot{u}_1}{\dot{u}_{1gr}} & \text{for } |\dot{u}_1| \le \dot{u}_{1gr} \end{cases} \tag{18}$$

where: Ats_1 is amplitude of the force of sliding friction in the suspension system and $\dot{u}_{1gr}$ is boundary value of the suspension system deflection rate, see (19):

$$\dot{u}_1 = \dot{\zeta}_2 - \dot{\zeta}_1 \tag{19}$$

The force of viscous damping in the suspension system is described by (20):

$$Ft_1 = \begin{cases} -i_z \cdot c_o \cdot (-\dot{u}_1 \cdot i_z)^{Wo} & \text{for } \dot{u}_1 < 0 \\ i_z \cdot c_u \cdot (\dot{u}_1 \cdot i_z)^{Wu} & \text{for } \dot{u}_1 \ge 0 \end{cases} \tag{20}$$

where: i_z is a coefficient describing the kinematic relations in the suspension system; c_0 and c_u are shock absorber damping coefficients for the rebound and compression stroke; Wo and Wu are exponents of the function that describes the shock absorber damping for the rebound and compression stroke.

The tire elasticity force was approximated by a 3rd degree polynomial:

$$Fs_2 = As_2 \cdot u_2^3 + Bs_2 \cdot u_2^2 + Cs_2 \cdot u_2 \tag{21}$$

where: As_2 to Cs_2 are coefficients of the polynomial that describes the tire elasticity force and u_2 is radial deflection

of the tire, according to (22):

$$u_2 = \begin{cases} \zeta - \zeta_2 + R & \text{for } \zeta - \zeta_2 + R \geq 0 \\ 0 & \text{for } \zeta - \zeta_2 + R < 0 \end{cases} \tag{22}$$

where: R is free radius of the pneumatic tire.

According to equation (23), the damping force in the tire model is a linear function of the rate of tire deflection in the radial direction:

$$Ft_2 = c_2 \cdot \dot{u}_2 \tag{23}$$

where: c_2 is damping coefficient and $\dot{u}_2$ is deflection rate, according to (24):

$$\dot{u}_2 = \begin{cases} \dot{\zeta} - \dot{\zeta}_2 & \text{for } \zeta - \zeta_2 + R \geq 0 \\ 0 & \text{for } \zeta - \zeta_2 + R < 0 \end{cases} \tag{24}$$

The solutions of the equations of motion (15) were obtained in the time domain by approximate techniques involving numerical integration, with using an authorial program built in the Matlab-Simulink environment [2].

4 Parameters of the models and of the test conditions

All the simulation tests were carried out for nominal parameters of the front and rear "quarter" of the selected medium-class car (Tables 1 and 2), which had been previously subjected to test rig measurements.

Table 1: Parameters of the linear model

Symbol	Unit	Value for the front "quarter car"	Value for the rear "quarter car"
m_1	kg	346	160
m_2	kg	36	35
k_1	N/m	25570	24882
k_2	N/m	253161	206526
c_2	N·s/m	150	150
f_{01} (ω_{01})	Hz (rad/s)	1.30 (8.19)	1.87 (11.77)
f_{02} (ω_{02})	Hz (rad/s)	14.01 (88.03)	12.96 (81.42)
c_{kr1}	N·s/m	5669	3770

In pursuance of the objective of this work, only the viscous damping in the suspension system was changed, with using the dimensionless (relative) coefficient (14) and with applying every time 12 values of this parameter, ranging from 0.04 to 0.48 (with $\Delta\vartheta_1 = 0,04$).

Table 2: Additional parameters of the nonlinear model and the diagnostic tester

Symbol	Unit	Value for the front "quarter car"	Value for the rear "quarter car"
$A1s_1$	N/m	2.267E+05	4.400E+05
$A2s_1$	N/m^3	0	7.290E+05
$B2s_1$	N/m^2	1.852E+04	−5.037E+04
$C2s_1$	N/m	2.310E+04	2.155E+04
$D2s_1$	N	1.526E+03	4.094E+02
u_{1gr}	m	0.0075	0.001
om_0	m	0.337	0.309
Ats_1	N	200	40
$\dot{u}_{1gr}$	m/s	0.005	0.005
c_u	$N{\cdot}s^{Wu}/m^{Wu}$	975	850
c_o	$N{\cdot}s^{Wo}/m^{Wo}$	1700	3200
Wu	-	0.8	0.65
Wo	-	1	1.2
i_z	-	0.9936	0.7068
As_2	N/m^3	−9.367E+07	−3.021E+07
Bs_2	N/m^2	5.653E+06	3.592E+06
Cs_2	N/m	1.525E+05	1.553E+05
R	m	0.311	0.311
m_3	kg	14.5	14.5
ζ_{max}	m	0.025 or 0.006	0.025 or 0.006

For the nonlinear model, the force of viscous damping in the suspension system was reproduced from the nominal characteristic curve, with multiplying it by a percentage factor appropriately selected so that the energy dissipated in a single cycle in the shock absorber being simulated was equal to that dissipated in the corresponding linear element of the model.

The analysis was focused on the factors of gain in the vertical force at the tire-exciter contact point (relative to the input force) and on the relative coefficients of viscous damping in the suspension system, determined by the half-power bandwidth method. The distortions caused by the force of exciter's inertia were also shown if deemed significant.

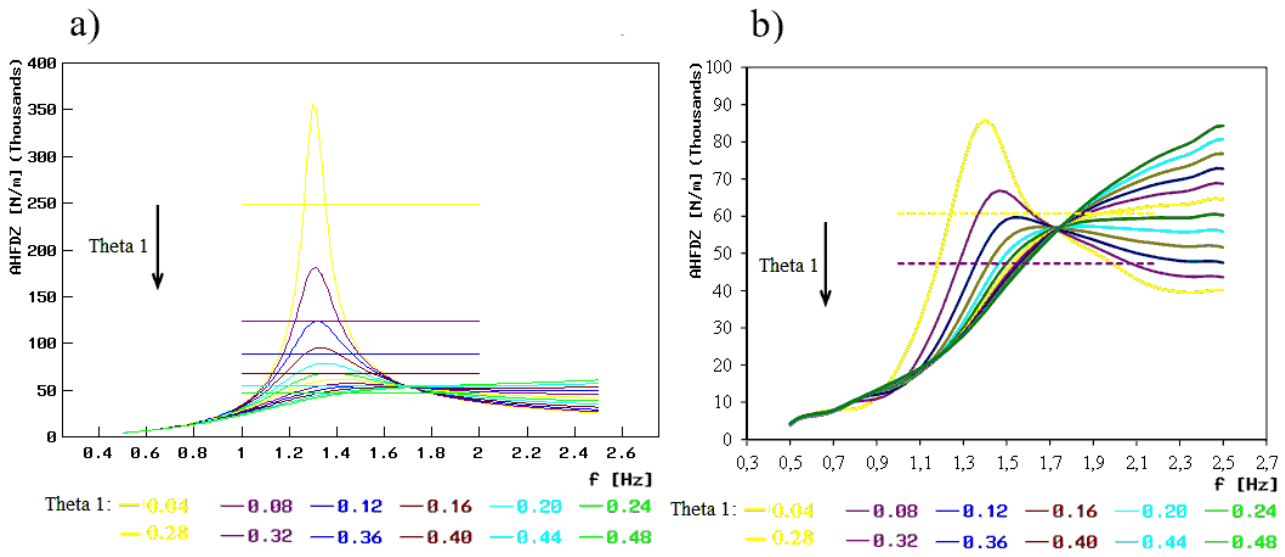

Figure 3: Factors of gain (AHFDZ) in the vertical force at the tire-exciter contact point (relative to the input force) close to the first natural frequency of the front "quarter car" for various damping values ϑ_1 (Theta1): The horizontal lines represent the values of $AHFDZ_{max}/\sqrt{2}$; a) results for the linear model; b) results for the nonlinear model

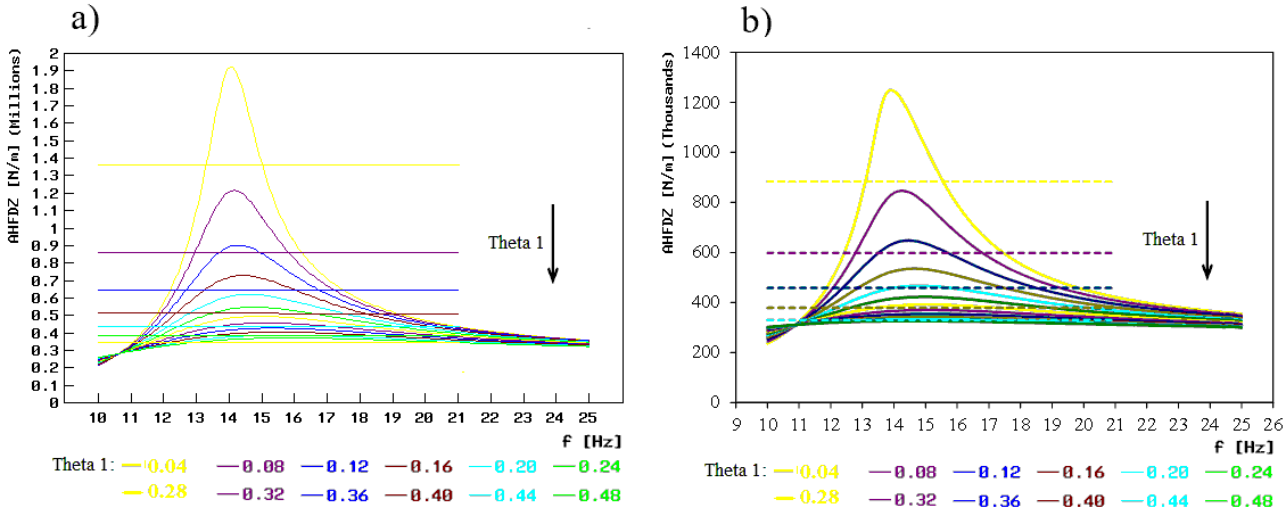

Figure 4: Factors of gain (AHFDZ) in the vertical force at the tire-exciter contact point (relative to the input force) close to the second natural frequency of the front "quarter car" for various damping values ϑ_1 (Theta1): the horizontal lines represent the values of $AHFDZ_{max}/\sqrt{2}$; a) results for the linear model; b) results for the nonlinear model

5 Results of simulation computations

The spectral characteristic curves obtained from the simulation tests carried out with using the linear model of the front "quarter car" were almost symmetrical, especially when the value of the dimensionless coefficient of damping in the suspension system did not exceed 0.24 (Figures 3a, 4a, and 5a). Close to the first natural frequency, the diagnostic parameters ϑ_{C1} and ϑ_{C2} (equations (1) and (2)) could be determined but only for the 6 lowest damping levels (of the range 0.04÷0.24). Close to the second natural frequency, in turn, the use of the half-power bandwidth method was reasonable in 7 of 12 cases. In contrast, the values of ϑ_{C1} and ϑ_{C2} could be estimated for all the damping levels under consideration (Figure 5a), if the factors of gain in the force under the tester's vibration plate (measured by means of real diagnostic testers) were used. For the calculations carried out with using the nonlinear model of the front "quarter car", the results obtained were less optimistic. The spectral characteristic curves showed some

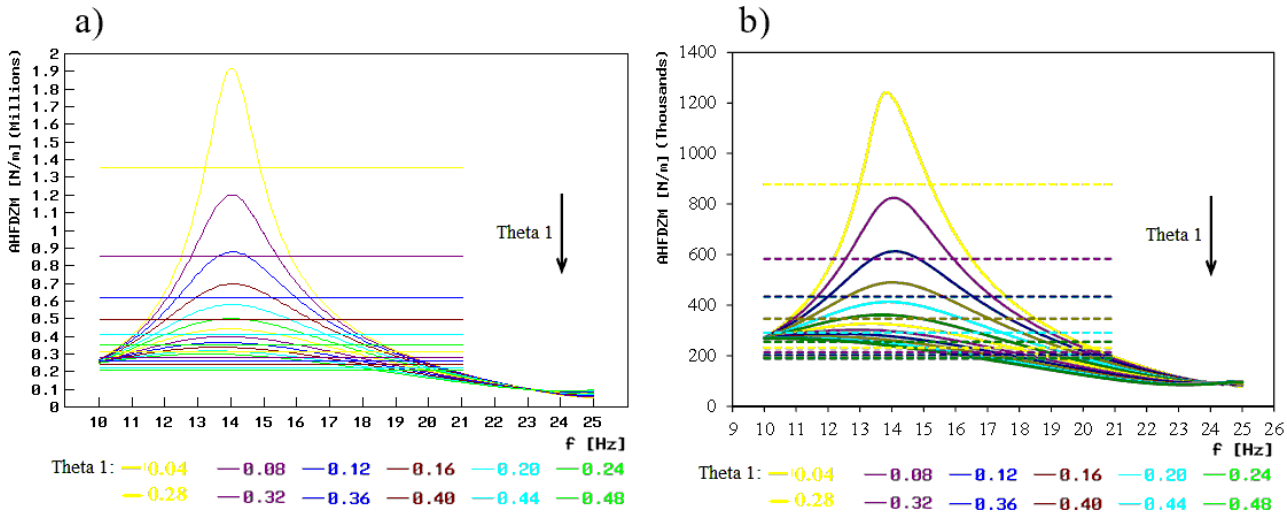

Figure 5: Factors of gain (AHFDZM) in the force measured by the real diagnostic tester, *i.e.* under the exciter (relative to the input force), close to the second natural frequency of the front "quarter car" for various damping values ϑ_1 (Theta1): the horizontal lines represent the values of $AHFDZ_{max}/\sqrt{2}$; a) results for the linear model; b) results for the nonlinear model

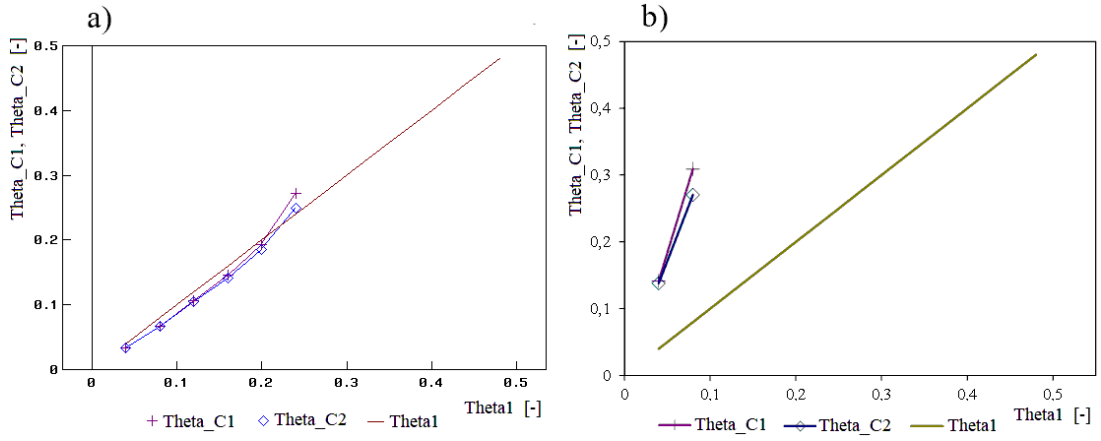

Figure 6: Values of diagnostic parameters ϑ_{C1} (Theta_C1) and ϑ_{C2} (Theta_C2) as functions of the dimensionless coefficient of damping in the suspension system ϑ_1 (Theta1), obtained from an analysis of the factor of gain in the vertical force at the tire-exciter contact point (relative to the input force) close to the first natural frequency of the front "quarter car": a) results for the linear model; b) results for the nonlinear model

symmetry, but only close to the second natural frequency. For the curves presented in Figures 3b, 4b, and 5b, the parameters ϑ_{C1m} and ϑ_{C2m} could only be estimated for the first 2, first 5, and all the damping levels in question, respectively.

The final simulation results, determined from the spectral characteristic curves close to the first natural frequency of the linear model corresponded to the applied values of the dimensionless coefficient of damping of the range 0.04÷0.24 (Figures 6a and 9a). For higher values of this coefficient, a trend to overestimate the values of ϑ_{C1} and ϑ_{C2} (even by about 25%) was noticed or the values could not be determined at all.

For the nonlinear model of the front "quarter car", in turn, high sliding friction forces in the suspension system prevented the obtaining of final test results except for the tests with the two lowest damping levels, where the results were several times overestimated at that (Figure 6b). Somewhat better results were obtained for the rear suspension system (Figure 8b). However, the ϑ_{C1} and ϑ_{C2} values could only be determined for the five lowest damping levels and the values corresponding to the levels of 0.04 and 0.2 were overestimated even by as much as several ten percent.

In the case of using the factors of gain in the vertical force at the tire-exciter contact point (relative to the input force) close to the second natural frequency of the

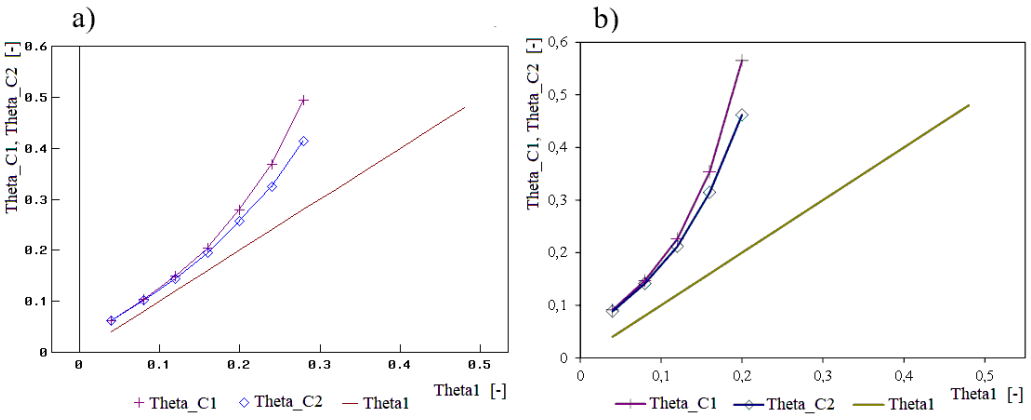

Figure 7: Values of diagnostic parameters ϑ_{C1} (Theta_C1) and ϑ_{C2} (Theta_C2) as functions of the dimensionless coefficient of damping in the suspension system ϑ_1 (Theta1), obtained from an analysis of the factor of gain in the vertical force at the tire-exciter contact point (relative to the input force) close to the second natural frequency of the front "quarter car": a) results for the linear model; b) results for the nonlinear model

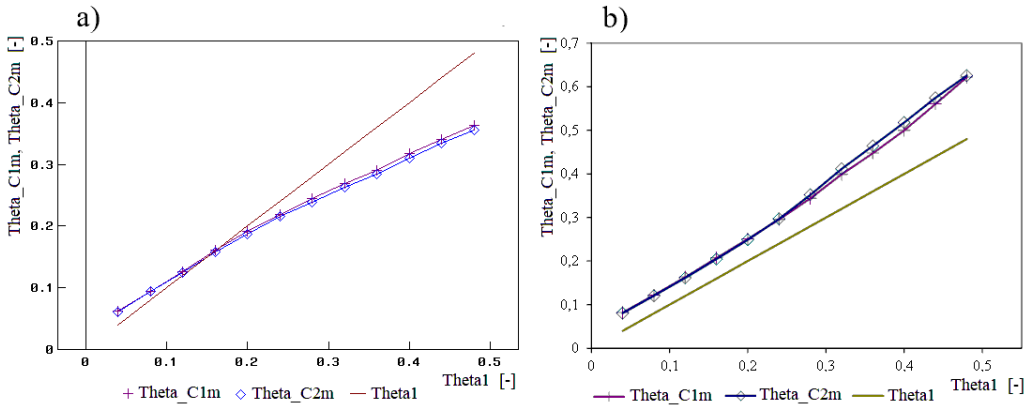

Figure 8: Values of diagnostic parameters ϑ_{C1m} (Theta_C1m) and ϑ_{C2m} (Theta_C2m) as functions of the dimensionless coefficient of damping in the suspension system ϑ_1 (Theta1), obtained from an analysis of the factor of gain in the force measured by the real diagnostic tester, *i.e.* under the exciter (relative to the input force), close to the second natural frequency of the front "quarter car": a) results for the linear model; b) results for the nonlinear model

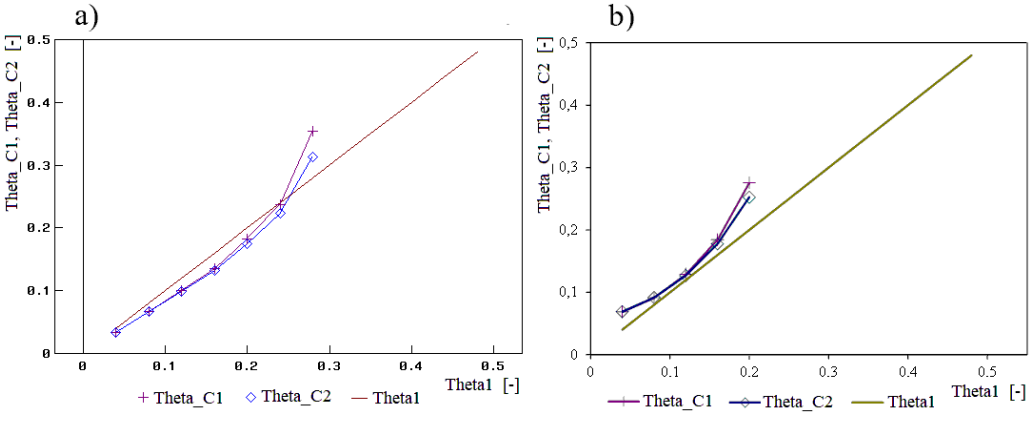

Figure 9: Values of diagnostic parameters ϑ_{C1} (Theta_C1) and ϑ_{C2} (Theta_C2) as functions of the dimensionless coefficient of damping in the suspension system ϑ_1 (Theta1), obtained from an analysis of the factor of gain in the vertical force at the tire-exciter contact point (relative to the input force) close to the first natural frequency of the rear "quarter car": a) results for the linear model; b) results for the nonlinear model

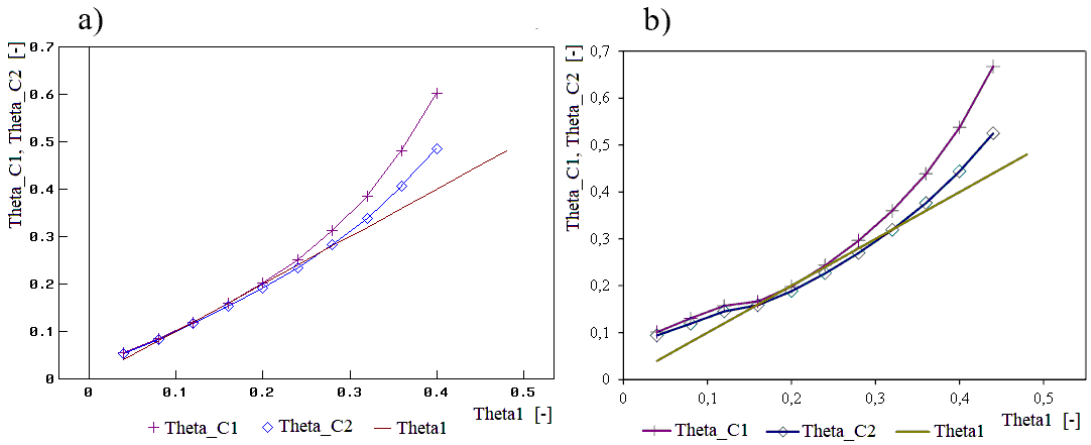

Figure 10: Values of diagnostic parameters ϑ_{C1} (Theta_C1) and ϑ_{C2} (Theta_C2) as functions of the dimensionless coefficient of damping in the suspension system ϑ_1 (Theta1), obtained from an analysis of the factor of gain in the vertical force at the tire-exciter contact point (relative to the input force) close to the second natural frequency of the rear "quarter car": a) results for the linear model; b) results for the nonlinear model

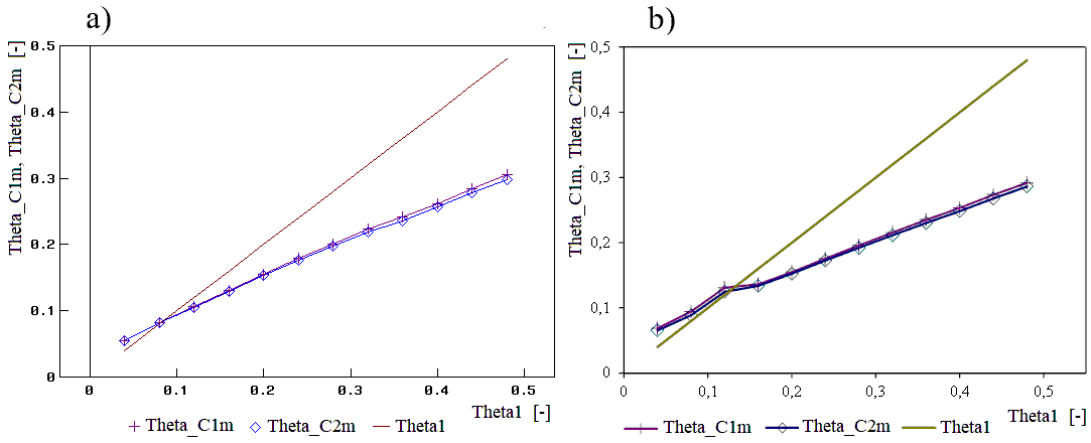

Figure 11: Values of diagnostic parameters ϑ_{C1m} (Theta_C1m) and ϑ_{C2m} (Theta_C2m) as functions of the dimensionless coefficient of damping in the suspension system ϑ_1 (Theta1), obtained from an analysis of the factor of gain in the force measured by the real diagnostic tester, *i.e.* under the exciter (relative to the input force), close to the second natural frequency of the rear "quarter car": a) results for the linear model; b) results for the nonlinear model

front "quarter car", quite good conformity was obtained between the final test results and the predefined values, but only when the latter were relatively low (Figures 7a and 10a). For the front suspension system, significant overestimation of parameters ϑ_{C1} and ϑ_{C2} (even by as much as several ten percent) was observed when the damping level exceeded 0.16. For the rear suspension system, the value of this threshold was 0.28.

For the nonlinear front "quarter car" model, the calculations produced test results overestimated by several ten to about two hundred percent in the whole range of changes in the damping (Figure 7b). The results obtained in this case were markedly better for the rear suspension system (Figure 10b). Parameters ϑ_{C1} and ϑ_{C2} adequately described the shock absorber condition, but only within the medium damping range. For very low and very high damping levels (0.04÷0.12 and above 0.36), the overestimation of the final test results reached a few ten percent. The phenomenon of tire separation from the exciter ("bouncing") resulted in conspicuous distortions of the initial parts of the curves plotted (Figures 10b and 11b).

Wherever the calculations made for the front "quarter car" were based on the factors of gain in the force measured under the tester's vibration plate, their results better represented the suspension damping applied, in comparison with the case that the vertical force at the tire-exciter contact point was taken as a basis (see Figures 7 and 8). For the linear model, the diagnostic parameters were gen-

erally underestimated (by up to about 25%); conversely, those obtained for the nonlinear representation remained overestimated, but definitely less than it can be seen in Figure 7b. A different situation was observed for the rear suspension system: here, the ϑ_{C1m} and ϑ_{C2m} values represented the suspension damping levels worse than ϑ_{C1} and ϑ_{C2} did and they were underestimated in most cases (see Figures 10 and 11).

6 Recapitulation

Based on the simulation tests carried out, the usability of the half-power bandwidth method in the diagnostic testing of automotive shock absorbers was found to be limited.

The final calculation results were approximately in conformity with expectations but in general, this was only true for low suspension system damping values. However, such cases, occurring when the shock absorbers are in poor condition, are most important in the practical applications of this method. At high damping levels, overestimation of the diagnostic parameters was usually observed, although different situations occurred as well.

A distorting impact of sliding friction in the suspension system on the final test results was noticed. The cases have also been shown where the new diagnostic parameters proposed cannot be determined at all.

The results presented indicate the usability of the linear model, although many important characteristics of a real object are not taken into account in such a model.

In authors' opinion, experimental verification of the results obtained is necessary because in practice, at low-frequency input (even if the input amplitude is raised to 12.5 mm), the extremum of the response of the system under test becomes hardly distinguishable. Moreover, the shock absorber under test usually fails to function in such conditions if the sliding friction in the suspension system is strong enough.

Acknowledgement: The work was done within project "*UNILINE QUANTUM (…)*" sponsored by the European Union within the European Regional Development Fund, Smart Growth Operational Programme, Sub-measure 1.1.1. Project No: POIR.01.01.01-00-0949/15. Task carried out by the authors for UNIMETAL Sp. z o.o. in Złotów.

References

[1] Stańczyk TL, Jurecki R. [Comparative analysis of testing methods of hydraulic shock absorbers]. Proceedings of the Institute of Vehicles, Warsaw University of Technology. 2014;4(100):25-45. Polish.

[2] Zdanowicz P. Assessment of vehicle shock-absorbers' condition having considered dry friction in the suspension [dissertation]. Warsaw: Warsaw University of Technology; 2012.

[3] Calvo JA, Diaz V, San Román JL. Establishing inspection criteria to verify the dynamic behaviour of the vehicle suspension system by a platform vibrating test bench. International Journal of Vehicle Design. 2005;38(4):290-306.

[4] Lozia Z, Zdanowicz P. Simulation assessment of the impact of inertia of the vibration plate of a diagnostic suspension tester on results of the EUSAMA test of shock absorbers mounted in a vehicle. IOP Conference Series: Materials Science and Engineering. 2018;421(2):1-10.

[5] Lozia Z, Mikołajczuk J. Ocena przydatności testu diagnostycznego stanu amortyzatorów zamontowanych w pojeździe, wykorzystującego wymuszenie kinematyczne w kontakcie koła z podłożem. The Archives of Automotive Engineering. 1997;2:3-24. Polish.

[6] Calvo JA, San Román JL, Alvarez-Caldas C. Procedure to verify the suspension system on periodical motor vehicle inspection. International Journal of Vehicle Design. 2013;63(1):1-17.

[7] He J, Fu ZF. Modal analysis. 1st ed. Woburn: Butterworth-Heinemann; 2001.

[8] Pugi L, Reatti A, Corti F. Application of modal analysis methods to the design of wireless power transfer systems. Meccanica. 2019;54:321–31.

[9] Lozia Z. The use of a linear quarter-car model to optimize the damping in a passive automotive suspension system – a follow-on from many authors' works of the recent 40 years. The Archives of Automotive Engineering. 2016;71(1):33-65.